EQUIVALENT STATIC LOADS FOR NONLINER SEISMIC DESIGN OF SPATIAL STRUCTURES

Jingyao Zhang[1], Makoto Ohsaki[2] and Atsushi Uchida[3]

[1] *Post-doctoral Research Fellow, Dept. of Architecture and Architectural Eng., Kyoto University, Japan*
[2] *Associate Professor, Dept. of Architecture and Architectural Eng., Kyoto University, Japan*
[3] *Graduate Student, Dept. of Architecture and Architectural Eng., Kyoto University, Japan*
Email: is.zhang@archi.kyoto-u.ac.jp, ohsaki@ archi.kyoto-u.ac.jp, is.uchida@archi.kyoto-u.ac.jp

ABSTRACT :

A new approach to determination of equivalent static seismic loads is presented for evaluating peak seismic responses. The responses are estimated by series of multi-modal pushover analysis considering possible phase differences in the dominant modes: the loads are directly applied in the elastic systems, and the damping due to plastic dissipation is modeled by equivalent linearization in inelastic systems. The accuracy of the proposed method is demonstrated in the numerical example of an arch-type long-span truss.

KEYWORDS: Multi-modal pushover analysis, Seismic response, Equivalent static load
Equivalent linearization, Inelastic response

1. INTRODUCTION

In the seismic design of structures, the peak values of responses such as displacements and base shear forces should be evaluated under possible earthquake excitations. Nonlinear static pushover analysis is commonly adopted to approximately estimate the seismic responses in practical design, instead of the Time-History Analysis (THA). Thus, the accuracy of static load pattern is the key to accurate estimation of the responses. There have been numerous studies on development of equivalent static loads for building frames, and the main purpose of this paper is to present a suitable load pattern for spatial structures for a given design response spectrum accounting for coupling of multiple vibration modes in dynamic responses.

For an elastic system, the peak response can be measured from the response spectrum for each dominant vibration mode, which are combined by the Square-Root-of-Sum-of-Squares (SRSS) rule (Rosenblueth, 1951), or by the Complete Quadratic Combination (CQC) rule (Rosenblueth and Elorduy, 1969; Der Kiureghian, 1981). For an inelastic system, these rules are not applicable, and three important problems arise in the static procedure: (1) how to deal with the vibration modes that are changed after plastification, (2) which modal combination rule to use, and (3) when to stop the increase of the loads.

For problem (1), several adaptive force distributions have been proposed to follow the time-variant distributions of inertia forces to provide better prediction; see for example Fajfar and Gaspersic (1996), Bracci *et al*. (1997), Gupta and Kunnath (2000). However, they are conceptually complicated and computationally inefficient, and we use the elastic vibration modes to define load pattern, based on the assumption that the distribution of inertia forces does not change suddenly after plastification.

For problem (2), some studies tried to find the optimal modal combination coefficients for dominant modes for building frames (Kunnath, 2004; Park *et al*., 2007). These coefficients, however, might not be optimal to other structures. In this study, we present a systematic way to determinate the coefficients considering possible phase differences between the dominant modes to obtain the snapshot of the response at maximum response.

Regarding problem (3), responses of elastic systems are estimated by directly applying the equivalent loads, and those of inelastic systems are estimated by the modified capacity spectrum method to account for multiple dominant modes.

2. EQUIVALENT STATIC SEISMIC LOAD

This section first identifies the vibration modes that dominate seismic response of a structure. A systematic way is then presented to combine the dominant vibration modes to derive the equivalent static seismic loads.

2.1. Dominant Vibration Modes

Behavior of a linear *N*-degrees-of-freedom system under ground motion $\ddot{u}_g(t)$ is governed by

$$\mathbf{M}\ddot{\mathbf{u}}(t)+\mathbf{C}\dot{\mathbf{u}}(t)+\mathbf{K}\mathbf{u}(t)=-\mathbf{M}\boldsymbol{\iota}\ddot{u}_g(t) \tag{1}$$

where $\mathbf{u}$ is a vector of nodal displacements relative to the ground; $\mathbf{M}$, $\mathbf{C}$ and $\mathbf{K}$ $(\in \mathbb{R}^{N\times N})$ are the mass, viscous damping and stiffness matrices of the system; $\boldsymbol{\iota}$ is the influence vector: 1 in the direction of motion and 0 for others. The nodal displacements $\mathbf{u}(t)$ can be written as sum of the modal displacements $\mathbf{u}_n(t)$

$$\mathbf{u}(t)=\sum_{n=1}^{N}\mathbf{u}_n(t), \quad \mathbf{u}_n(t)=\Gamma_n D_n(t)\boldsymbol{\Phi}_n \tag{2}$$

$$\Gamma_n=\frac{\boldsymbol{\Phi}_n^{\mathrm{T}}\mathbf{M}\boldsymbol{\iota}}{M_n}, \quad M_n=\boldsymbol{\Phi}_n^{\mathrm{T}}\mathbf{M}\boldsymbol{\Phi}_n \tag{3}$$

where $\boldsymbol{\Phi}_n$, Γ_n and M_n are respectively the vibration mode, modal participation factor and generalized mass, and $D_n(t)$ is the *n*th modal displacement defined by the circular natural frequency ω_n and damping ratio h_n.

The dominant modes can be identified by the effective mass ratio ρ_n or the maximum strain energy E_n:

$$\rho_n=\frac{M_n}{M}, \quad E_n=\frac{1}{2}M_n\left(\omega_n\hat{D}_n\right)^2 \tag{4}$$

where M is the total weight of the structure, $\hat{D}_n$ is the peak value in $D_n(t)$, or it is readily available from the displacement response spectrum. For the responses defined by the specific design spectra, E_n is more reliable than Γ_n and ρ_n, because it incorporates the characteristics of the seismic motions (Kato *et al*. 2007).

2.2. Load Pattern

For a linear system, the displacements $\mathbf{u}_n(t)$ corresponding to the *n*th mode at the specific time can be computed by the following pseudo-static equation against the equivalent static external loads $\mathbf{f}(t)$:

$$\mathbf{f}_n(t)=\mathbf{K}\mathbf{u}_n(t) \tag{5}$$

Substituting $\mathbf{u}_n(t)=\Gamma_n D_n(t)\boldsymbol{\Phi}_n$ into the above equation, applying $\mathbf{K}\boldsymbol{\Phi}_n=\omega_n^2\mathbf{M}\boldsymbol{\Phi}_n$ and denoting the invariant external forces by $\mathbf{s}_n=\Gamma_n\mathbf{M}\boldsymbol{\Phi}_n$ and pseudo-acceleration by $A_n(t)=\omega_n^2 D_n(t)$, we have

$$\mathbf{f}_n(t)=\mathbf{K}\mathbf{u}_n(t)=\mathbf{K}(\Gamma_n D_n(t)\boldsymbol{\Phi}_n)=(\omega_n^2 D_n(t))(\Gamma_n\mathbf{M}\boldsymbol{\Phi}_n)=A_n(t)\mathbf{s}_n \tag{6}$$

For the case where pseudo-acceleration response spectrum $\hat{A}_n$ is available, its corresponding static load is

$$\hat{\mathbf{f}}_n=\hat{A}_n\mathbf{s}_n \tag{7}$$

Suppose that *m* lowest vibration modes dominate seismic response of a structure. It is unlikely that all the *m* dominant modes reach their peak responses at the same time. Therefore, to obtain the snapshot of the peak deformation, a weighted sum of these static loads is defined as

$$\mathbf{f}=\sum_{n=1}^{m}\alpha_n\hat{\mathbf{f}}_n \tag{8}$$

where α_n is the modal coefficient for the *n*th mode.

For a linear system, the peak modal displacements $\hat{\mathbf{u}}_n$ can be directly computed as follows from Eq. (2)

$$\hat{\mathbf{u}}_n=\Gamma_n\hat{D}_n\boldsymbol{\Phi}_n=\frac{\Gamma_n\hat{A}_n}{\omega_n^2}\boldsymbol{\Phi}_n \tag{9}$$

Suppose that the dominant modes vibrate in full amplitudes around the time of peak deformation of the

structure. From Eqn. (9), α_n is determined by finding the time $t_{\max}$, at which c reaches its peak

$$c = \sum_{n=1}^{m} \pm c_n \sin(\omega_n t - \theta_n) = \sum_{n=1}^{m} \pm \frac{\Gamma_n \widehat{A}_n}{\omega_n^2} \sin(\omega_n t - \theta_n) \tag{10}$$

within the time period $0 \le t \le \pi/\omega_1$, where θ_n is the phase angle of the *n*th mode. As will be interpreted later in the numerical example, the sign for each mode relies on the modal shape. The coefficients are then given as

$$\alpha_n = \sin(\omega_n t_{\max} - \theta_n) \tag{11}$$

Since the phase angles are random values, various possible phase differences should be considered; the mean value of the static responses by the different loads is taken as the estimated peak response of the structure.

Fig. 1 shows a simple example illustrating how to derive the modal combination coefficients. Two sinusoidal functions with amplitudes $c_1 = 2.0$, $c_2 = 1.0$, periods $2\pi/\omega_1 = 2.0(s)$, $2\pi/\omega_2 = 1.0(s)$ and phase angles $\theta_1 = 0^o$, $\theta_2 = 30^o$ are plotted in the figure. The signs corresponding to modes 1 and 2 are assumed to be positive; the sum of the two functions within the time period $0 \le t \le 1.0(\text{sec})$ arrives its peak at time $t_{\max} = 0.4(\text{sec})$. The coefficients are then computed by Eqn. (12) as $\alpha_1 = 0.951$, $\alpha_2 = 0.914$.

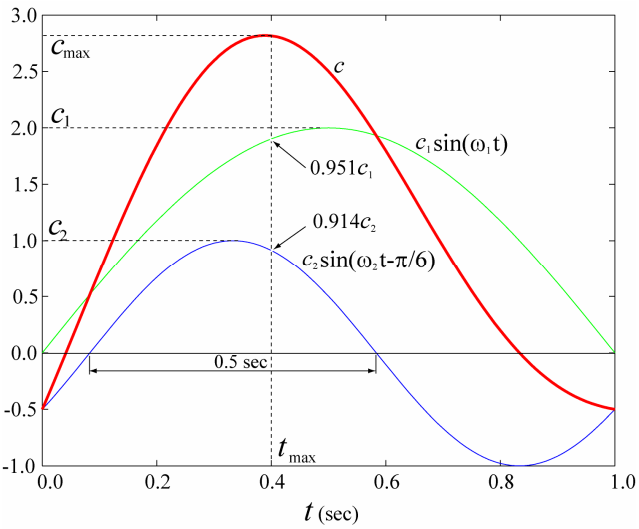

Figure 1. Computation of modal combination coefficients.

3. RESPONSE OF INELASTIC SYSTEMS

In an elastic system, the peak response is determined directly as follows by applying the equivalent static loads:

$$\hat{\mathbf{u}} = \sum_{n=1}^{m} \alpha_n \hat{\mathbf{u}}_n = \sum_{n=1}^{m} \alpha_n \frac{\Gamma_n \widehat{A}_n}{\omega_n^2} \boldsymbol{\Phi}_n \tag{12}$$

In an inelastic system, however, the use of the same procedure will overestimate the response because of the reduced stiffness and increased damping due to plastification. To incorporate the effect of plastification, the capacity spectrum method (CSM) (Chopra and Goel, 1999; Freeman, 2004) is adopted here with modification to account for multiple dominant vibration modes. Moreover, we insist that the equivalent load is a weighted sum of the elastic modes to keep the procedure as simple as that for the elastic system, although the deformed shape will no longer follow exactly the combined modal shapes in inelastic range after plastification. The concept of CSM is illustrated in Fig. 2: it compares the capacity (diagram) of the structure converted from the pushover curve, with demands (diagram) on the structure, in the form of an elastic response spectrum.

3.1. Capacity Diagram

Suppose that the displacements $\mathbf{u}^i$ and equivalent accelerations $\mathbf{a}^i$, at step *i* of the pushover process using the equivalent loads, are written as a linear combination of the dominant vibration modes

$$\mathbf{u}^i = \sum_{n=1}^{m} {}_u c_n^i \boldsymbol{\Phi}_n, \quad \mathbf{a}^i = \sum_{n=1}^{m} {}_a c_n^i \boldsymbol{\Phi}_n, \quad \text{where} \quad \hat{\mathbf{f}}_n^{\,i} = \mathbf{M}\mathbf{a}^i \tag{13}$$

Using the orthogonality property of the vibration modes, the coefficients can be computed as

$${}_u c_n^i = \boldsymbol{\Phi}_n{}^{\mathrm{T}} \mathbf{M}\mathbf{u}^i, \quad {}_a c_n^i = \boldsymbol{\Phi}_n{}^{\mathrm{T}} \mathbf{M}\mathbf{a}^i \tag{14}$$

Moreover, similarly to $\mathbf{u}(t)$ and $\mathbf{u}_n(t)$ in Eqn. (2), we write $\mathbf{u}^i$ as

$$\mathbf{u}^i = \sum_{n=1}^{m} \Gamma_n D_n^i \boldsymbol{\Phi}_n, \quad \mathbf{a}^i = \sum_{n=1}^{m} \Gamma_n A_n^i \boldsymbol{\Phi}_n \tag{15}$$

Substituting Eqn. (14) into Eqn. (15) and using the orthogonality property of the vibration modes, we have

$$D_n^i = \frac{{}_u c_n^i}{\boldsymbol{\Phi}_n{}^{\mathrm{T}} \mathbf{M}\boldsymbol{\iota}} = \frac{{}_u c_n^i}{\Gamma_n M_n}, \quad A_n^i = \frac{{}_a c_n^i}{\boldsymbol{\Phi}_n{}^{\mathrm{T}} \mathbf{M}\boldsymbol{\iota}} = \frac{{}_a c_n^i}{\Gamma_n M_n} \tag{16}$$

The generalized displacement and acceleration in the capacity diagram are defined as

$$D^i = \sqrt{\sum_{n=1}^{m} (D_n^i)^2}, \quad A^i = \sqrt{\sum_{n=1}^{m} (A_n^i)^2} \tag{17}$$

The equivalent natural frequency is computed by

$$T_{eq} = \sqrt{A^i / D^i} \tag{18}$$

3.2. Demand Diagram

The demand diagram is also in the (psudo-)acceleration-displacement format. The post-yielding behavior is accounted for by equivalent viscous damping. To compute the equivalent damping ratio, we need to idealize the bi-linear capacity diagram as a linear system, as shown in Fig. 3. (D_y, A_y) is the yielding point, and ω_{eq}, γ and μ are the equivalent natural frequency, equivalent hardening ratio and ductility ratio, respectively. For the equivalent damping ratio h_{eq}, we adopt the model in ATC-40:

$$h_{eq} = h_0 + \kappa h, \quad h = \frac{2}{\pi} \frac{(\mu - 1)(1 - \gamma)}{\mu(1 + \gamma\mu - \gamma)} \tag{19}$$

where h_0 and h are respectively the inherent viscous damping ratio and the equivalent hysteretic damping ratio, and κ is the damping modification factor dependent on the types of hysteretic behavior of the system and the equivalent damping ratio. There are in total three types of system considered in ATC-40: Type A denotes hysteretic behavior with stable and full hysteresis loops; Type C represents severely pinched loops; and the hysteretic behavior of the Type system is between Type A and Type C. The demand diagram is updated as

$$A = F \times G \times A_0 \tag{20}$$

where A_0 is the elastic acceleration spectrum, F is the coefficient depending on the damping ratio, and G is the coefficient representing the ground property.

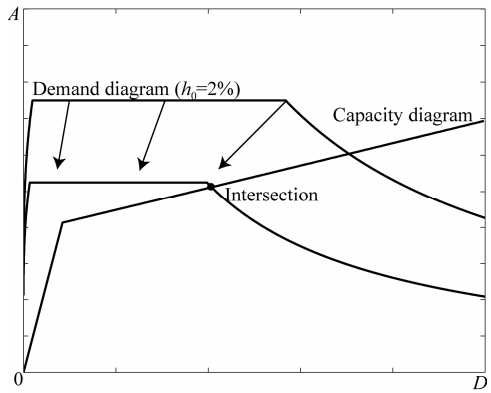

Figure 2. Concept of the capacity spectrum method.

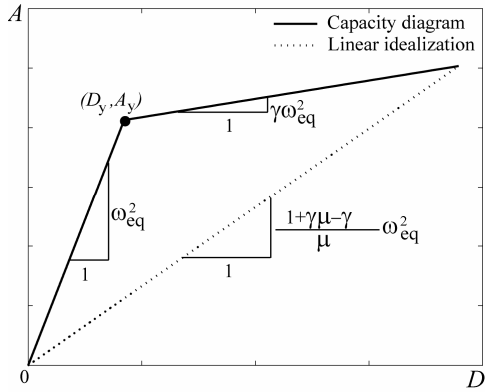

Figure 3. Linear idealization of the capacity diagram.

3.3. Analysis Procedure

The peak responses are approximated as follows by the equivalent static external forces:

Step 1: Plot the pushover curve by the equivalent static seismic loads, and convert it into capacity diagram using Eqn.(17). Plot the demand diagram in terms of displacement and pseudo-acceleration for damping ratio h_0.

Step 2: Use the first secant of the capacity diagram to find its intersection with the demand diagram to determine the peak displacement D_j and the corresponding pseudo-acceleration A_j.

Step 3: Calculate the equivalent damping ratio h_{eq} from Eqn. (20) and ductility by $\mu = D_j / D_y$.

Step 4: Plot the demand diagram for h_{eq}, and find its intersection with the capacity diagram to read-off D_{j+1} and A_{j+1}.

Step 5: If $(D_{j+1} - D_j)/D_{j+1}$ is sufficiently small, then terminate the iteration and approximate response is $\mathbf{u}^i$, where its corresponding quantity D^i satisfies $D^i = D_{j+1}$; otherwise, let $j := j+1$ and go to Step 3.

4. NUMERICAL EXAMPLE

4.1. Arch Model

We consider the arch model in Fig. 4. It represents one bay of a spatial structure that is widely used for school gymnasiums. The model consists of a cylindrical roof and two support columns. The span is 80 m, and the column height is 3.5 m. The lower nodes of the arch are located on a circle with radius of 80 m, and the half-open angle is 20 degrees. Both of the height of the roof truss and width of the column trusses are 1/40 of the span. The distance between two bays of the structure in the longitudinal direction is supposed to be 8 m.

The members of the arch are steel pipes modeled as truss elements. The weight of the roof and the external walls are assigned as 0.98 kN/m^2 and 1.47 kN/m^2, respectively. The masses are lumped at the external nodes of the columns and the upper nodes of the roof. Young•s modulus is 2.05×10^{11} N/m^2. For the inelastic system, the steel materials are idealized by a bilinear constitutive model with yield stress 2.35×10^{8} N/m^2, and hardening coefficient 1/100. The effect of geometrical nonlinearity is not considered in this study.

The arch is subjected to horizontal motion. The values of T_n, Γ_n, ρ_n and E_n for the five lowest modes are listed in Table 1. It can be observed that the 1st and 3rd modes plotted in Fig. 5 dominate in the seismic response, since the sum of E_n corresponding to these two modes exceeds 95% of the total maximum strain energy, moreover, the values of Γ_n and ρ_n of these modes are much larger than any other modes.

The peak displacements d_1, d_2, d_3, d_4, d_5 at the nodes A, B, C, and reaction forces F_1, F_2 at node D as indicated in Fig. 4 are to be estimated. FEDEASLab by Filippou and Constantinides (2004), a MATLAB analysis program, is used for static and dynamic analyses in the study.

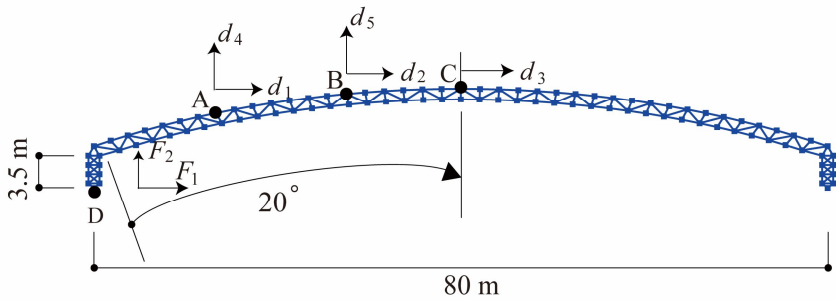

Figure 4. The arch model; the horizontal displacements d_1, d_2, d_3, base shear force F_1 and vertical displacements d_4, d_5, base shear force F_2 are to be evaluated.

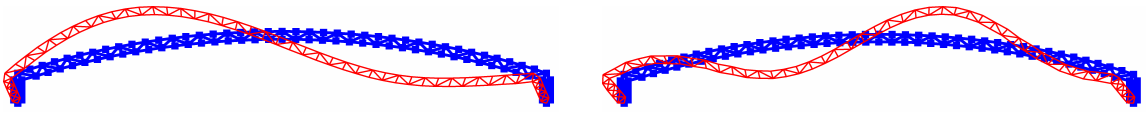

(a) 1st vibration mode (b) 3rd vibration mode

Figure 5. The 1st and 3rd vibration modes of the arch model.

Table 1. The natural period T_n, modal participation factor Γ_n, ratio of effective mass ρ_n and maximum strain energy E_n of the five lowest vibration modes.

Mode n	T_n	Γ_n	ρ_n	E_n
1	1.34	0.602	0.34	6.19×10^4
2	1.14	0.0	0.0	0.0
3	0.45	0.698	0.46	3.02×10^4
4	0.42	0.0	0.0	0.0
5	0.26	0.316	0.09	0.42×10^4

4.2. Load Patterns

The phase angle of the first vibration mode is fixed at $\theta_1 = 0.0$, while θ_3 is varied as $i\pi/8$ $(i = 1,...8)$. The sign in Eqn. (11) is defined to be consistent with the signs of the mode components corresponding to each displacement or acceleration to be evaluated. Thus, we have the following two patterns:

Load pattern 1: $c = c_1 \sin\omega_1 t + c_3 \sin(\omega_3 t - \theta_3)$ for d_1, d_2, d_3 and F_1

Load pattern 2: $c = c_1 \sin\omega_1 t - c_3 \sin(\omega_3 t - \theta_3)$ for d_4, d_5 and F_2

The combination coefficients α_1 and α_3 are listed in Table 2, where there are eight cases for each load pattern corresponding to the different phase angles of the 3rd mode; i.e., $\theta_3 = i\pi/8$ $(i = 1,...8)$.

Table 2. Modal combination coefficients.

Pattern	Phase	1	2	3	4	5	6	7	8
1	α_1	0.83	0.86	0.88	0.92	0.95	0.98	0.99	1.00
	α_3	0.26	0.49	0.70	0.77	0.84	0.90	0.98	1.00
2	α_1	1.00	1.00	0.99	0.97	0.94	0.92	0.88	0.86
	α_3	-1.00	-0.98	-0.95	-0.91	-0.85	-0.69	-0.61	-0.39

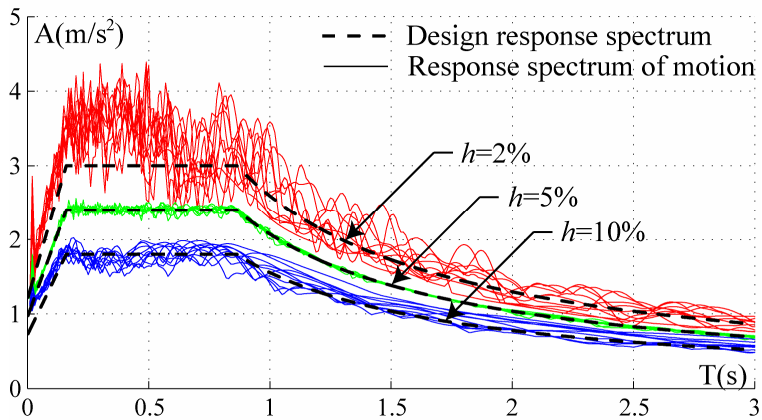

Figure 6. Design pseudo-acceleration spectra for h=2%, 5%, 10% damping and response spectra of the artificial seismic motions.

4.3. Prediction Accuracy

Ten artificial seismic motions are generated by the standard superposition method of sinusoidal waves (Scanlan and Sachs, 1974), where the phase difference spectrum of El-Centro 1940(EW) has been used. The target spectrum is the design acceleration response spectrum for 5% damping specified by Notification 1461 of the Ministry of Land, Infrastructure and Transport (MLIT), Japan, corresponding to the performance level of life safety. The amplification factor G for the ground of 2nd rank and the definition of F defined in Notification 1457 of MLIT is used. The pseudo-acceleration spectra for h=2%, 5%, 10% damping, together with the design response spectra, are plotted in Fig. 6.

Table 3. Mean and standard deviation of the estimation ratios for elastic system.

	Horizontal direction (Load pattern 1)				Vertical direction (Load pattern 2)		
Response	d_1	d_2	d_3	F_1	d_4	d_5	F_2
Mean	0.98	0.98	0.99	0.87	0.91	0.99	0.79
St. dev.	0.098	0.096	0.105	0.195	0.056	0.089	0.152

In the THA, the Rayleigh damping is adopted with h = 0.02 for the 1st and 3rd modes, and the time step for integration by the Newmark-β method (β = 1/4) is 0.01 sec. The estimation ratio of each monitored response, defined as ratio of the predicted peak value to the value by THA, is used as accuracy measure.

In the elastic system, the peak response is estimated by Eqn. (12). The mean values and standard deviations of estimation ratios are summarized in Table 3. It is observed that the proposed method is of high accuracy for estimation of peak seismic responses for elastic systems.

The inelastic arch model is a Type C system with $\kappa = 0.33$ in ATC-40, because the structure consists of slender members. Table 4 lists the result of the proposed method for each loading cases. T_{eq}, h_{eq}, μ, $A_{\max}$ and $D_{\max}$ are the quantities at the intersection of the capacity and demand diagrams. The mean values and standard deviations of the estimation ratios corresponding to each monitored response are summarized in Table 5. The proposed method underestimates the response d_4, and has good estimation for other responses.

Table 4. Results of nonlinear static analyses for the eight loading cases.

Pattern	Phase	A_y (m/s^2)	D_y (m)	T_{eq} (s)	h_{eq} (%)	μ	$A_{\max}$ (m/s^2)	$D_{\max}$ (m)
1	1	4.74	0.140	1.353	14.6	1.93	5.82	0.270
	2	4.61	0.110	1.268	15.6	2.22	6.00	0.244
	3	4.53	0.092	1.218	17.1	2.41	5.89	0.221
	4	4.51	0.089	1.212	17.3	2.45	5.88	0.219
	5	4.48	0.087	1.206	17.5	2.50	5.87	0.216
	6	4.50	0.086	1.200	17.6	2.49	5.86	0.214
	7	4.48	0.083	1.192	17.8	2.54	5.86	0.211
	8	4.48	0.083	1.193	17.8	2.55	5.86	0.211
2	1	13.99	0.353	1.034	3.4	1.08	14.10	0.382
	2	13.87	0.355	1.035	3.2	1.07	13.97	0.379
	3	13.74	0.356	1.045	3.3	1.08	13.86	0.384
	4	13.62	0.360	1.058	3.4	1.08	13.73	0.389
	5	13.41	0.363	1.069	3.4	1.08	13.52	0.391
	6	12.45	0.376	1.140	3.7	1.10	12.57	0.414
	7	12.10	0.379	1.157	3.6	1.09	12.21	0.414
	8	10.82	0.409	1.286	4.0	1.12	10.89	0.456

Table 5. Mean and standard deviation of the estimation ratios for inelastic system.

	Horizontal direction (Load pattern 1)				Vertical direction (Load pattern 2)		
Response	d_1	d_2	d_3	F_1	d_4	d_5	F_2
Mean	1.02	1.04	1.09	0.98	0.77	0.92	0.90
St. dev.	0.046	0.042	0.033	0.014	0.043	0.025	0.096

5. CONCLUSIONS AND DISCUSSIONS

A systematic approach has been presented for deriving the equivalent static loads for estimation of peak seismic response of elastic as well as inelastic structures for given design response spectrum. Multiple dominant modes are incorporated in the form of weighted sum of the elastic vibration modes. Several sets of modal combination coefficients are determined by considering phase differences of the peak modal responses. The peak response of an elastic system can be computed directly by applying the equivalent external loads; and that of an inelastic system is estimated by conducting pushover analysis until the demand and capacity diagrams intersect.

Numerical studies on a long-span arch model, of which the seismic response is dominated by two vibration modes, show that the proposed method has good performance in estimating the peak responses for elastic systems as well as inelastic systems. Although the proposed method requires eigenvalue analysis and pushover analysis for several load patterns, it is effective and accurate enough for estimating peak seismic responses of spatial structures, as an alternative tool of the time-consuming time-history analysis.

REFERENCES

Applied Technology Council (1996). Seismic evaluation and retrofit of concrete buildings. Report ATC 40. November.

Bracci J.M., Kunnath S.K. and Reinhorn A.M. (1997). Seismic performance and retrofit evaluation for reinforced concrete structures. *Journal of Structural engineering, ASCE* **123:1**, 3-10.

Chopra A.K. and Goel R.K. (1999). Capacity-demand-diagram methods for estimating seismic deformation of inelastic structures: SDF systems; Report No. PEER-1999/02.

Der Kiureghian A. (1981). A response spectrum method for random vibration analysis of MDF systems, *Earthquake Engineering and Structural Dynamics* **9**, 419-435.

Fajfar P. and Gaspersic P. (1996). The N2 method for the seismic damage analysis of RC buildings, *Earthquake Engineering & Structural Dynamics* **25:1**, 31-46.

Filippou F.C. and Constantinides M. (2004). FEDEASLab getting started guide and simulation examples. Technical Report NEESgrid-2004-22, Department of Civil and Environmental Engineering, Unversity of California, Berkeley.

Freeman S.A. (2004). Review of the development of the capacity spectrum method, *ISEL Journal of Earthquake Technology* **41:1**, 1-13.

Gupta B. and Kunnath S.K. (2000). Adaptive spectra-based pushover procedure for seismic evaluation of structures. *Earthquake Spectra* **16:2**, 367-392.

Kato S., Nakazawa S. and Saito K. (2007). Estimation of static seismic loads for latticed domes supported by substructure frames with braces deteriorated due to buckling, *J. IASS*, **48:2**, 71-86.

Kunnath S.K. (2004). Identification of modal combinations for nonlinear static analysis of building structures, *Computer-Aided Civil and Infrastructure Engineering* **19**, 246-259.

Park H.G., Eom T. and Lee H. (2007). Factored modal combination for evaluation of earthquake load profiles, *Journal of Structural Engineering, ASCE* **133:7**, 956-968.

Rosenblueth E. (1951). A Basis for Aseismic Design, Ph.D. thesis, University of Illinois, Urbana, Ill.

Rosenblueth E. and Elorduy J. (1969). Responses of linear systems to certain transient disturbances, *Proc. of the 4th World Conference on Earthquake Engineering*, Santiago, Chile, Vol. I, 185-196.

Scanlan R.H. and Sachs K. (1974). Earthquake time histories and response spectra, *Proc. ASCE*, **100(EM4)**, 635-655.